(CH_2Cl_2) ν_{CO} 1920, 1850 cm^{-1}. Anal. Calcd for $C_{24}H_{19}MnPO_2$: C, 67.61; H, 4.73. Found: C, 67.65; H, 4.92.

X-ray Data Collection, Structure Determination and Refinement for $(\eta^5\text{-}C_5H_5)(CO)_2[(\eta^5\text{-}C_5H_5)[\eta^5\text{-}C_5H_4P(C_6H_5)_2]TiCl_2]Mn$ (6). A crystal of **6** suitable for X-ray analysis was grown by carefully layering hexane onto a solution of **6** in methylene chloride. The resulting mixture was allowed to stand undisturbed for ca. 48 h, whereby diffusional mixing of the two layers had taken place, effecting the formation of purple crystals. Single crystals of the air-sensitive compound were sealed under N_2 in thin-walled glass capillaries. Final lattice parameters as determined from a least-squares refinement of $((\sin\theta)/\lambda)^2$ values for 15 reflections ($\theta > 20°$) accurately centered on the diffractometer are given in Table I. Systematic absences allowed the space group to be either *Pnma* or $Pn2_1a$. Subsequent structure solution and refinement in the centrosymmetric *Pnma* showed this to be the correct choice.

Data were collected on an Enraf-Nonius CAD-4 diffractometer by the θ-2θ scan technique. The method has been previously described.[25] A summary of the data collection parameters is given in Table I. The intensities were corrected for Lorentz and polarization effects, but not for absorption.

Calculations were carried out with the SHELX system of computer programs.[26] Neutral atom scattering factors for Ti, Mn, Cl, P, O, and C were taken from Cromer and Waber,[27] and the scattering for titanium and manganese were corrected for the real and imaginary components of anomalous dispersion using the table of Cromer and Liberman.[28] Scattering factors for H were from ref 29.

The positions of the titanium, manganese, and chlorine atoms were revealed by the direct methods program MULTAN.[30] A difference Fourier map phased on these atoms revealed some disorder about the mirror plane in the centrosymmetric *Pnma*. Refinement in the noncentrosymmetric $Pn2_1a$ produced high correlations between atoms that were properly related by the mirror (O(1), C(1), C(2), and C(3)). The *R* factor for anisotropic refinement of all nonhydrogen atoms in $Pn2_1a$ was 0.135 and a difference Fourier map revealed peaks corresponding to the $CpPPh_2$ and the other Cp ligand on titanium as related by a mirror plane. The correct choice was then taken to be *Pnma* with Ti, Mn, Cl(1), Cl(2), and C(2) in the plane, O(1), C(1), C(3) and C(4) correctly related by the mirror, and all the other atoms disordered about the mirror plane with occupancy factors of 0.5. The two exceptions are atoms C(21) and C(22). These atoms would not refine off the mirror plane, and thus distortion is noted in the bond distances and angles involving these two atoms. Some disorder about the plane was noted for Cl(1) and Cl(2), but it could not be resolved. Least-squares refinement with isotropic thermal parameters led to $R = \sum||F_o| - |F_c||/\sum|F_o| = 0.178$. The hydrogen atoms could not be located due to the nature of the disorder, and their contributions were therefore not included in the first refinement. Refinement with anisotropic temperature factors led to final values of $R = 0.073$ and $R_w = 0.072$. A final difference Fourier showed no feature greater than 0.4 $e^-/Å^3$. The weighting scheme was based on unit weights; no systematic variation of $w(|F_o| - |F_c|)$ vs. $|F_o|$ or $(\sin\theta)/\lambda$ was noted. The final values of the fractional coordinates are given in Table II. The final values of the thermal parameters are available as supplementary materials.[31] Bond distances and angles for **6** are given in Table III.

Acknowledgment. We are grateful to the National Science Foundation (Grant CHE-8018210 to M.D.R. and Grant CHE-8111137 to J.L.A.) as well as to the donors of the Petroleum Research Fund, administered by the American Chemical Society (Grant 12593-ACl to M.D.R.), for support of this research program.

Registry No. 1, 58109-48-1; **2**, 85320-10-1; **3**, 1270-98-0; **4**, 85320-11-2; **5**, 85320-12-3; **6**, 85320-13-4; **7**, 85320-14-5; **8**, 85320-15-6; chlorodiphenylphosphine, 1079-66-9; (cyclopentadienyl)thallium, 34822-90-7.

Supplementary Material Available: A listing of thermal parameters, and observed and calculated structure factors (10 pages). Ordering information is given on any current masthead page.

(25) Holton, J.; Lappert, M. F.; Ballard, D. G. H.; Pearce, R.; Atwood, J. L.; Hunter, W. E. *J. Chem. Soc., Dalton Trans.* **1979**, 46.
(26) SHELX, a system of computer programs for X-ray structure determination by G. M. Sheldrick, 1976.
(27) Cromer, D. T.; Waber, J. T. *Acta Crystallogr.* **1965**, *18*, 104.
(28) Cromer, D. T.; Liberman, D. *J. Chem. Phys.* **1970**, *53*, 1891.
(29) "International Tables for X-ray Crystallography", Kynoch Press: Birmingham, England, 1974; Vol. IV, p 72.
(30) Germain, G.; Main, P.; Woolfson, M. M. *Acta Crystallogr., Sect. A* **1971**, *A27*, 368.
(31) See paragraph at the end of paper regarding supplementary material.

Carbon Dioxide Activation by Lithium Metal. 1. Infrared Spectra of $Li^+CO_2^-$, $Li^+C_2O_4^-$ and $Li_2^{2+}CO_2^{2-}$ in Inert-Gas Matrices

Z. H. Kafafi, R. H. Hauge, W. E. Billups, and J. L. Margrave*

Contribution from the Department of Chemistry and Rice Quantum Institute, Rice University, Houston, Texas 77251. *Received October 6, 1982*

Abstract: Lithium atoms react spontaneously with carbon dioxide to form $Li^+CO_2^-$ and $Li_2^{2+}CO_2^{2-}$ in inert gas matrices. Reaction of Li and CO_2 in an argon matrix leads also to the formation of $Li^+C_2O_4^-$. Two geometrical isomers of $Li^+CO_2^-$ have been isolated in solid argon. One has a ring structure in which the metal interacts symmetrically with the two oxygen atoms, while in the second isomer the lithium atom is bonded to only one of the two oxygens. It is found that $Li^+CO_2^-(C_s)$ rearranges upon photolysis with a Nernst glower IR source to the symmetric $Li^+CO_2^-(C_{2v})$. Similarly, $Li^+C_2O_4^-$ photolytically converts to an $LiCO_2$:CO_2 adduct. $Li_2^{2+}CO_2^{2-}$ is produced under high concentration of the alkali metal as a result of the reaction of dilithium or two lithium atoms with carbon dioxide. Lithium oxalate ($Li_2C_2O_4$) is formed in concentrated matrices. For the first time, all three expected intraionic infrared-active modes of CO_2^- as well as a Li^+-CO_2^- interionic mode have been identified for both $Li^+CO_2^-$ geometrical isomers. Isotopic shifts have been measured for lithium-6-, carbon-13-, and oxygen-18-enriched products. A CO_2^- valence bond angle equal to 125.7° has been calculated. Normal coordinate analyses have been carried out on $LiCO_2(C_{2v})$ and $LiCO_2(C_s)$ by using 22 and 30 measured frequencies, respectively, for all the isotopomers of the two geometrical isomers.

Introduction

In the search for new catalytic processes that may lead to the conversion of cheap available CO_2 into organic compounds, there have been many investigations of ways of activating the CO_2 molecule whether by coordination with transition metals[1,2] or transition-metal complexes,[3] by insertion into M-H, M-C, M-N, and M-O bonds,[3-16] or by electron transfer with an electron source

(1) H. Huber, D. McIntosh, and G. A. Ozin, *Inorg. Chem.*, **16**, 975 (1977).
(2) G. A. Ozin, H. Huber, and D. McIntosh, *Inorg. Chem.*, **17**, 1472 (1978).
(3) I. S. Kolomnikov and M. Kh. Grigoryan, *Russ. Chem. Rev.*, **47**, 334 (1978).

0002-7863/83/1505-3886$01.50/0

such as an electric current, photocells, or reducing agents.[17]

The reduction of CO_2 to the radical anion CO_2^- thus represents an important mode of activation. CO_2^- was first produced in alkali halide matrices by γ irradiation of sodium formate.[18] The ESR, the ultraviolet, and the infrared spectra of the radical have been reported, and a valence angle of 127 ± 8° has been estimated on the basis of the carbon-13 shift of the asymmetric CO_2 stretching frequency. The decay half-life of this radical in a KBr disk at room temperature was estimated to be over a year. Hartman and Hisatsune[19] have studied the kinetics of the pyrolysis of the oxalate ion and have suggested that the rate-determining step involves a unimolecular dissociation of $C_2O_4^{2-}$ into $2CO_2^-$ species. Under anhydrous conditions CO_2^- was found to disproportionate into CO_3^{2-} and CO or combine to form $C_2O_4^{2-}$.[20]

The radical anion has also been formed on a rotating cryostat by alternatively depositing Na or K and CO_2 at 77 K.[21,22] The electron affinity of CO_2 has been experimentally determined[23] to be −0.6 ± 0.2 eV by the collisional ionization of an alkali metal such as Na, K, and Cs by CO_2. The vibrational spectrum of CO_2^- was also obtained in an argon matrix at 14 K.[24] A valence bond angle close to 130° has been calculated for CO_2^-. The ESR spectrum of the $LiCO_2$ complex in solid CO_2 at 77 K indicated that the Li 2s electron is strongly localized on CO_2.[25] Rotation of CO_2^- around the O–O axis above 8 K was suggested from the measured axial symmetry of the spectroscopic and hyperfine tensors. The spectrum of $LiCO_2$ was found to disappear at 150 K with the growth of a new signal that was assigned to small lithium clusters.

Theoretical calculations of the stabilities and geometries of Li–CO_2 and Na–CO_2 complexes have been carried out recently.[26] Two planar structures that are close in energy (0.83 vs. 0.85 eV) have been proposed for $LiCO_2$. One is a rhombic structure where the Li and CO_2 are in a cyclic arrangement with Li interacting equally with both oxygen atoms. The other structure consists of a Li atom bonded to one of the two oxygens. Corresponding nonplanar structures were found to lie at a higher energy.

The radical anion CO_2^- and the dianion CO_2^{2-} have been recently detected as reactive intermediates in solid Xe and CO_2 in the lithium-induced reductive coupling of carbon dioxide.[27] IR spectra of $Li^+CO_2^-$, $Li_2^{2+}CO_2^{2-}$ and $Li_2C_2O_4$ were observed in solid xenon, but only $Li^+CO_2^-$ and $Li_2C_2O_4$ were produced in CO_2 matrices, suggesting that lithium oxalate is formed via the dimerization of $LiCO_2$. In an attempt to learn more about the chemistry of these systems, the mechanisms of the above reactions, and the new species formed, the following study has been undertaken as an extension of the previous work.[27]

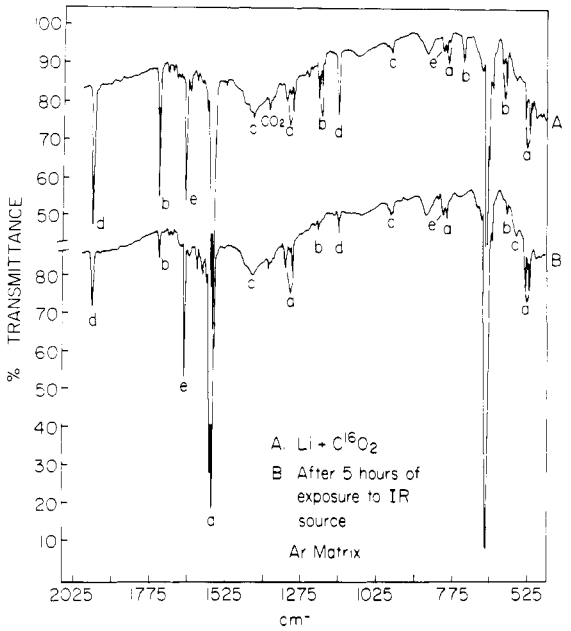

Figure 1. Infrared spectra of products from reactions of lithium with carbon dioxide in an argon matrix: (A) spectrum measured immediately after 1-h deposition; (B) spectrum measured after 5 h of exposure to the Nernst glower source; a = $LiCO_2(C_{2v})$, b = $LiCO_2(C_s)$, c = $Li_2CO_2(C_s)$, d = $LiC_2O_4(C_{2v})$, and e = $Li_2C_2O_4(D_{2h})$.

Experimental Section

Lithium metal was vaporized from a stainless steel crucible by resistively heating the tantalum furnace in the temperature range 350–480 °C. The atomic beam of lithium was then co-deposited with carbon dioxide in an excess of an inert gas onto a polished copper surface. After trapping for a period of 1 h, the copper mirror was rotated 180° and the infrared reflection spectrum was measured with a Beckman IR-9 spectrophotometer. A closed-cycle helium refrigerator was used for cooling the copper block to the desired temperature (15 K). The rates of deposition of lithium, carbon dioxide, and the inert gas used were measured with a quartz crystal microbalance. Vaporization temperatures of lithium were determined by using an alumel–chromel thermocouple affixed to the effusion cell. The flow rates of the inert gas and carbon dioxide were independently monitored through two needle valves connected to thermocouple gauges.

Lithium metal of high purity (99%) was obtained from Alfa Inorganics. An isotopically enriched sample of the metal (96% in ^6Li) was furnished by the Oak Ridge National Laboratory. Carbon dioxide (99.8%) and enriched samples containing 98% of $C^{18}O_2$ and 90% of ^{13}CC hased from Matheson Gas Products, Prochem Isotopes Ltd., anto Research Corp., respectively. $C^{18}O^{16}O$ was synthesi ng $C^{18}O_2$ over hot lithium carbonate that was placed in a Pyı rounded by a chromel wire and resistively heated to the temperature range 500–550 °C. The lithium carbonate, obtained from J. T. Baker Chemical Co., was dried in the oven, then heated and pumped on overnight in the Pyrex tube prior to the experiment. Matheson argon (99.99%) was further purified by passing it through hot titanium. Krypton (99.99%) and xenon (99.99%), obtained from Matheson Gas Products and from Cryogenic Rare Gas Laboratories, respectively, were used without further purification. Nitrogen purchased from Matheson Gas Products Co. was allowed to pass through a liquid-nitrogen trap during deposition. Carbon dioxide was passed through a dry ice bath to remove any volatile gases present as impurities.

Photolysis of the matrices occurred by exposure of the copper surface to the Nernst glower IR source with or without a quartz filter that has an infrared cutoff at ~3000 cm^{-1}. All spectra were calibrated against H_2O, CO_2, and NH_3 lines in the different infrared regions. Absolute frequencies were measured to an accuracy of ±0.5 cm^{-1}. A detailed description of the matrix isolation apparatus has been given in earlier publications.[28,29]

(4) M. Aresta and C. F. Nobile, *J. Chem. Soc., Dalton Trans.*, **708** (1977).
(5) T. Ito and A. Yamamoto, *J. Chem. Org. Synth. Jpn.*, *34*, 308 (1976).
(6) T. Herskowitz and J. J. Guggenberger, *J. Am. Chem. Soc.*, **98**, 1615 (1976).
(7) A. Miyashita and A. Yamamoto, *J. Organomet. Chem.*, **113**, 187 (1976).
(8) M. Aresta and C. F. Nobile, *Inorg. Chim. Acta*, **24**, L49 (1977).
(9) R. Eisenberg and D. E. Hendriksen, *Adv. Catal.*, **28**, 79 (1979).
(10) S. Komiya and A. Yamanoto, *Bull. Chem. Soc. Jpn.*, **49**, 784 (1976).
(11) A. Immirzi and A. Musco, *Inorg. Chim. Acta*, **22**, L35 (1977).
(12) T. Yoshida, Y. Ueda, and S. Otsuka, *J. Am. Chem. Soc.*, **100**, 3941 (1978).
(13) A. D. English and T. Kerskowitz, *J. Am. Chem. Soc.*, **99**, 1648 (1977).
(14) T. Tsuda, Y. Chujo, and T. Saegusa, *J. Am. Chem. Soc.*, **100**, 630 (1978).
(15) T. V. Ashworth and E. Singleton, *J. Chem. Soc., Chem. Commun.*, 204 (1976).
(16) M. H. Chisholm, F. A. Cotton, M. W. Extine, and W. W. Reichert, *J. Am. Chem. Soc.*, **100**, 1727 (1978).
(17) M. Pasquali, C. Floriani, A. Chiesi-Villa, and C. Guastini, *J. Am. Chem. Soc.*, **101**, 4740 (1979); *Inorg. Chem.*, **20**, 349 (1981).
(18) K. O. Hartman and I. C. Hisatsune, *J. Chem. Phys.*, **44**, 1913 (1966).
(19) K. O. Hartman and I. C. Hisatsune, *J. Phys. Chem.*, **71**, 392 (1967).
(20) I. C. Hisatsune, T. Adl, E. C. Beahm, and R. J. Kempf, *J. Phys. Chem.*, **74**, 3225 (1970).
(21) B. Mile, *Angew. Chem., Int. Ed. Engl.* **7**, 507 (1968).
(22) J. E. Bennett, S. C. Graham, and B. Mile, *Spectrochim. Acta, Part A*, **29A**, 375 (1973).
(23) R. N. Compton, P. W. Reinhardt, and C. D. Cooper, *J. Chem. Phys.*, **63**, 3821 (1975).
(24) M. E. Jacox and D. E. Milligan, *Chem. Phys. Lett.*, **28**, 163 (1974).
(25) J. P. Borel, F. Faes, and P. Pittet, *J. Chem. Phys.*, **74**, 2120 (1981).
(26) Y. Yoshioka and K. D. Jordan, *Chem. Phys. Lett.*, **84**, 370 (1981).
(27) R. H. Hauge, J. L. Margrave, J. W. Kauffman, N. A. Rao, M. M. Konarski, J. P. Bell, and W. E. Billups, *J. Chem. Soc., Chem. Commun.*, 1258 (1981).

Results

Five different sets of bands have been recorded upon the co-condensation of lithium metal with carbon dioxide in excess argon. These absorption bands have been labelled a–e in Figure 1 and include four main infrared regions, namely, the C=O, C–O, and Li–O stretching regions and the δ(OCO) bending region. Mole ratios between Li and CO_2 varied from 4:1 to as low as 1:25 while Li:Ar was about 1:~250 in most experiments. When the matrix was exposed to the Nernst glower source for 5 h, the intensities of the b and d bands considerably decreased while the a bands became much stronger along with side features to some of these bands. This behavior is illustrated in Figure 1B and suggests that species b and d photolytically convert to a. Similar behavior was observed but at a much slower rate when a quartz filter with an infrared cutoff at ~3000 cm^{-1} was utilized during photolysis.

Absorption bands a and b shown in Figure 1 were predominant under low concentrations of both Li and CO_2 while species c was present at a Li:CO_2 ratio of 4:1 and was favored by a higher metal concentration. On the other hand the d bands were prominent at a CO_2:Li ratio of about 2.5:1, indicating that this species contains more than one CO_2. High concentrations of both Li and CO_2 favored the formation of species e.

There are four sets of bands associated with molecule a. The first set of bands lies in the C=O or CO_2 asymmetric stretching region. There are two main absorption bands at 1568.6 and 1569.9 cm^{-1}, respectively, with two small shoulders at 1561.9 and 1564.4 cm^{-1}. The absorption band at 1574.9 cm^{-1} is most prevalent under higher concentrations of CO_2 and is attributed to the "solvated" a species. The 1561.9- and 1574.9-cm^{-1} bands grow more rapidly than the other three bands upon irradiation with the Nernst glower IR source. The second set of peaks has absorptions at 1329.9, 1325.0, and 1304.9 cm^{-1}. The lowest frequency band is the counterpart of the 1574.9-cm^{-1} band. The third set of bands shows peaks at 798.7 and 807.0 cm^{-1}, respectively. Again the 807.0-cm^{-1} band is the counterpart of the 1304.9- and 1574.9-cm^{-1} bands since it is prominent under high CO_2 concentration. Two strong peaks and a middle weaker one that lie at 520.0, 533.4, and 526.0 cm^{-1}, respectively, form the last set of bands for this molecule. The 526.0-cm^{-1} band grows more rapidly than the other two bands upon irradiation with the Nernst glower source.

Similarly, molecule b has peaks in all four regions, and all of them except the one in the δ(OCO) bending region exhibit a doublet structure. The frequencies associated with this species are 1755.7, 1750.9, 1221.4, 1208.7, 739.5, 611.6, and 599.3 cm^{-1}. The splitting of these bands is probably due to different matrix sites occupied by this molecule.

Species c exhibits absorptions in only three main regions, namely, the C–O and the Li–O stretching regions at 1447.9, 984.2, and 565.9 cm^{-1}. No splitting is observed for these bands except in the infrared spectrum of the products from reaction of Li with $C^{18}O_2$.

Molecule d shows absorption in the C=O stretching region at 1968.7 cm^{-1} and in the C–O stretching region at 1159.8 cm^{-1}. Finally, four bands at 1662.2, 1315.5, 807.0, and 497.7 cm^{-1} are associated with species e. Note that contributions for the 807-cm^{-1} absorption are simultaneously made from species a and e.

Reactions of Li with $^{13}CO_2$, $^{12}CO_2$, and $^{12}CO_2/^{13}CO_2$ in argon matrices resulted in the infrared spectra shown in Figure 2. The 1568.8-cm^{-1} peak shifted by 40 cm^{-1} while the 1329.9-cm^{-1} band only moved by 26 cm^{-1}, thus implying that carbon motion is more involved in the higher frequency mode. A 9.6-cm^{-1} shift was measured for the 798.7-cm^{-1} band, and no shift was recorded for any of the lower frequency peaks at 520.0, 533.4, and 526.0 cm^{-1}.

Similar carbon-13 shifts were recorded for species b, namely, 43.9, 16.8, 9.1, and 3.0 cm^{-1} for the predominant bands in the four different infrared regions. Shifts of 52.2 and 7.5 cm^{-1} were measured for the higher and lower frequencies of the d absorption bands. From the mixed Li:$^{12}CO_2/^{13}CO_2$ reaction, it is clear that molecules a, b, and c have only one carbon while d and e contain

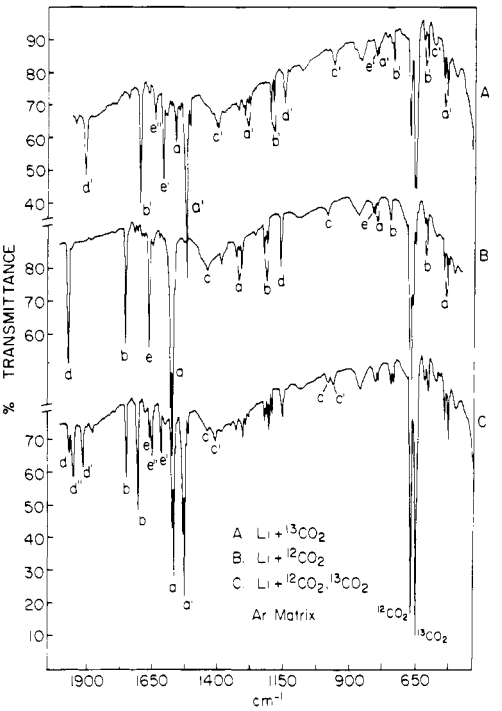

Figure 2. Infrared spectra of products from reactions of lithium with $^{13}CO_2$ (A), $^{12}CO_2$ (B), and $^{12}CO_2/^{13}CO_2$ (C) in solid argon; Li:$^{12}CO_2$:$^{13}CO_2$ is 1:1.2:1.5; a and a′ = $LiCO_2$ and $Li^{13}CO_2(C_{2v})$, b and b′ = $LiCO_2$ and $Li^{13}CO_2(C_s)$, c and c′ = Li_2CO_2 and $Li_2{}^{13}CO_2(C_s)$, d, d′, and d″ = LiC_2O_4, $Li^{13}C_2O_4$, and $Li^{12}C^{13}CO_4$, e, e′, and e″ = $Li_2C_2O_4$, $Li_2{}^{13}C_2O_4$, and $Li_2{}^{12}C^{13}CO_4$.

two equivalent carbon atoms as illustrated by the intensity patterns (1:2:1) of the absorption bands in Figure 2C. Note that in both molecules d and e, the frequency of the mixed $^{12}C/^{13}C$ species is much closer to that of the pure ^{12}C than that of the pure ^{13}C species, e.g., 1952.8 cm^{-1} for $^{12}C/^{13}C$ vs. 1968.7 and 1916.5 cm^{-1} for pure ^{12}C and ^{13}C and 1652.1 cm^{-1} for $^{12}C/^{13}C$ vs. 1662.2 and 1618.5 cm^{-1} for pure ^{12}C and ^{13}C.

Figure 3 presents the infrared absorption spectra obtained upon the co-condensation of a beam of lithium atoms with $C^{18}O_2$ (A), $C^{16}O_2$ (B), and $C^{16}O_2/C^{18}O_2/C^{18}O^{16}O$ (C) in solid argon. Oxygen-18 isotopic shifts of 27.7, 47.9, 32.1, and 2.7 cm^{-1} were measured for the 1568.6-, 1329.9-, 798.7-, and 553.4-cm^{-1} bands of species a, respectively. Note that the 1329.9- and 798.7-cm^{-1} absorptions involve the largest shifts,which reflects the fact that these vibrational modes involve more of the motion of the two oxygen atoms.

Isotopic shifts equal to 32.6, 41.1, 26.7, and 5.5 cm^{-1} were recorded for the 1750.9-, 1221.4-, 739.5-, and 599.3-cm^{-1} bands of the b species. A strange effect was observed for species c upon oxygen-18 substitution, and this was the splitting of all its bands into two sets of absorption bands that lie at 1412.6, 1418.5, 963.2, 968.8, 559.4, and 567.6 cm^{-1}. From the Li:$C^{18}O_2/C^{16}O_2/C^{18}O^{16}O$ mixed study, one concludes that species a contains two equivalent oxygen atoms as seen from the 1:2:1 triplet pattern while b has two nonequivalent oxygen atoms as reflected from the 1:1:1:1 quartet. A quartet pattern is also exhibited by c, but the frequencies of the mixed $^{18}O/^{16}O$ isotopic molecules are close to those of the pure ^{18}O and ^{16}O so the pattern appears to be a doublet. Thus c also contains two nonequivalent oxygens. The complexity of the patterns of the d and e bands suggests that these species are formed with at least two CO_2 molecules. When unscrambled equal amounts of $C^{18}O_2$ and $C^{16}O_2$ are co-condensed with lithium-6, one obtains bands at 1969.1, 1958.0, and 1937.4 cm^{-1} that exhibit a 1:2:1 pattern, thus proving that species d contains two equivalent CO_2 molecules.

From the above analysis, one concludes that species a and b contain one Li, and C, and two O's, the difference between a and b being that a has equivalent O's while b does not. Species c must have two Li's, one C, and two nonequivalent O's. Species d consists

(28) Z. K. Ismail, Ph.D. Thesis, Rice University, 1972.
(29) J. W. Kauffman, Ph.D. Thesis, Rice University, 1981.

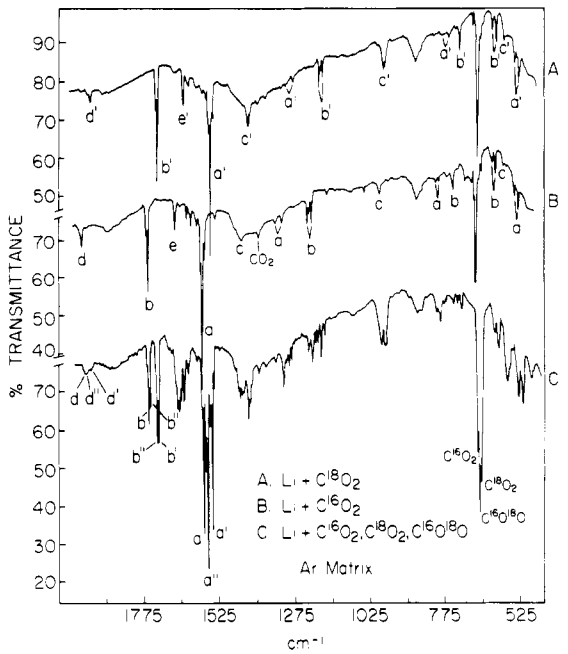

Figure 3. Infrared spectra of products from reactions of lithium with $C^{18}O_2$ (A), $C^{16}O_2$ (B), and $C^{16}O_2/C^{18}O_2/C^{18}O^{16}O$ (C) in an argon matrix: a, a', and a'' = $LiCO_2$, $LiC^{18}O_2(C_{2v})$, and $LiC^{18}O^{16}O(C_s)$; b, b', and b'' = $LiCO_2$, $LiC^{18}O_2$, and $LiC^{18}O^{16}O(C_s)$; c and c' = Li_2CO_2 and $Li_2C^{18}O_2(C_s)$; d, d', and d'' = LiC_2O_4 and $LiC_2{}^{18}O_4(C_{2v})$, and $LiC_2{}^{18}O_2{}^{16}O_2(C_s)$; e and e' = $Li_2C_2O_4$ and $Li_2C_2{}^{18}O_4(D_{2h})$.

Table I. Reaction Product Absorptions (cm^{-1}) for Li + CO_2 in Ar at 15 K

frequencies[a]	assignment
497.7 m	$Li_2C_2O_4$
520.0 m, 526.0 w, 533.4 m	$LiCO_2(C_{2v})$
565.9 w, br	Li_2CO_2
599.3 m, 611.6 m, br	$LiCO_2(C_s)$
739.5 m	$LiCO_2(C_s)$
798.7 w	$LiCO_2(C_{2v})$
807.0 w, br	$LiCO_2$:CO_2 and $Li_2C_2O_4$
984.2 w, br	Li_2CO_2
1159.8 m	LiC_2O_4
1208.7 m, 1221.4 m	$LiCO_2(C_s)$
1304.9 w, br	$LiCO_2$:CO_2
1315.5 w, br	$Li_2C_2O_4$
1325.0 w, br, 1329.9 w	$LiCO_2(C_{2v})$
1447.9 m, br	Li_2CO_2
1561.9 sh, 1564.4 sh, 1568.6 vs, 1569.9 vs	$LiCO_2(C_{2v})$
1574.9 s	$LiCO_2$:CO_2
1662.2 s	$Li_2C_2O_4$
1750.9 vs, 1755.7 m	$LiCO_2(C_s)$
1968.7 s	LiC_2O_4

[a] w, weak; m, medium; s, strong; vs, very strong; br, broad; sh, shoulder.

of one Li, two C's, and two sets of equivalent O's, while e has two Li's, two C's, and four O's.

Table I lists all of the measured frequencies for the product absorption bands from the reaction of lithium with carbon dioxide in solid argon at 15 K. Reactions of lithium with carbon dioxide in other matrices such as Kr, Xe, and N_2 lead only to the formation of one geometrical isomer of $LiCO_2$, Li_2CO_2, and $Li_2C_2O_4$. A typical infrared spectrum of the reaction products of Li with $C^{18}O_2/C^{16}O_2/C^{18}O^{16}O$ in a xenon matrix is shown in Figure 4A. Typical Xe:CO_2 mole ratios varied from 60:1 to 120:1, whereas Li:CO_2 were in the range of 4–1.3:1. When the matrix was allowed to warm up to room temperature (~300 K), the spectrum was taken of the residue left after the vaporization of Xe and excess CO_2 and is shown in Figure 4B. One notices the disappearance of the $LiCO_2$ and Li_2CO_2 bands, the growth of new absorption bands assigned to Li_2CO_3, and the increase in intensity of the

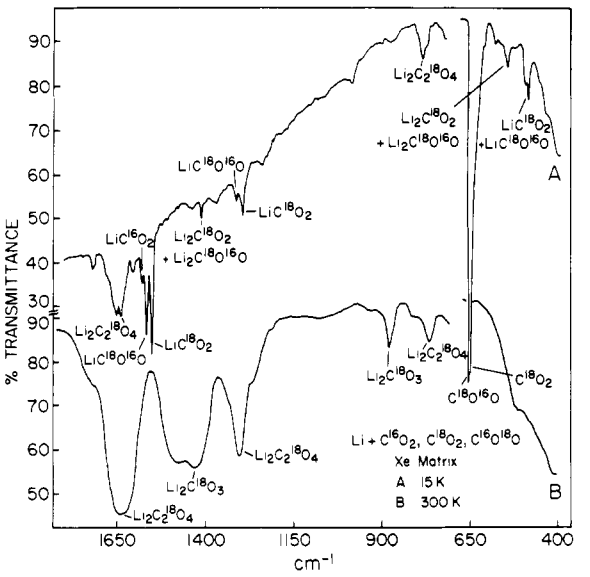

Figure 4. Infrared spectra of products from reactions of lithium with a mixture of $C^{16}O_2/C^{18}O_2/C^{18}O^{16}O$ in a xenon matrix at 15 K (A) and at room temperature (B).

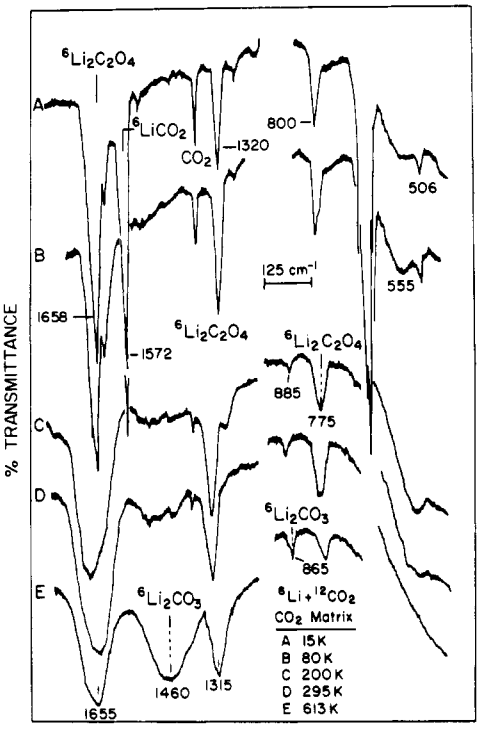

Figure 5. Infrared spectra of products from reactions of lithium with carbon dioxide in a neat matrix. Spectra were recorded as the matrix surface warmed from 15 to 613 K in vacuum.

$Li_2C_2O_4$ bands. A more cautious stepwise heating of the matrix from 15 to 600 K resulted in the spectra shown in Figure 5 for the reactions of lithium-6 with CO_2 in a neat matrix. Initially one notices the increase of the 1610-cm^{-1} absorption band associated with the "solvated" $LiCO_2$ and the decrease of the $LiCO_2$ peak at 1572 cm^{-1}. CO_2 is then lost via vaporization, and $LiCO_2$ disappears along with the excess CO_2. At 200 K only lithium oxalate remains. Further heating of the oxalate causes conversion to lithium carbonate, which is indicated by a growth of the broad 1460-cm^{-1} band.

Discussion

(A) Reactions of Lithium with Carbon Dioxide. (1) In an Argon Matrix. Co-condensation of lithium atoms with carbon dioxide in solid argon led to the formation of five products, namely, $LiCO_2(C_{2v})$, $LiCO_2(C_s)$, Li_2CO_2, LiC_2O_4, and $Li_2C_2O_4$. The yield

Table II. Comparison between Observed and Calculated Frequencies (cm^{-1}) for $LiCO_2(C_{2v})$ Isotopomers in Argon

vibr in-plane mode	$LiCO_2$		$^6LiCO_2$		$Li^{13}CO_2$		$^6Li^{13}CO_2$		$LiC^{18}O_2$		$^6LiC^{18}O_2$		$LiC^{18}O^{16}O$	
	obsd	calcd	obsd	calcd	obsd	calcd	obsd	calcd	obsd	calcd	obsd	calcd	obsd	calcd
$\nu_4(B_2)$, CO	1574.9[a]		1575.0[a]		1534.3[a]		1534.8[a]		1547.0[a]		1547.5[a]		1562.7[a]	
	1569.9	1570.9	1570.5	1570.9	1529.9	1529.6	1530.3	1529.7	1542.7	1541.9	1543.1	1541.9	1557.1	1557.7
	1568.6		1569.1		1528.3		1528.9		1540.9		1541.6		1555.2	
$\nu_1(A_1)$, CO	1329.9	1326.6	1328.1	1326.7	–	1305.1	1302.0	1305.1	1282.0	1284.0	1282.1	1284.1	–	1304.1
	1304.9[a]		1305.1[a]		1280.7[a]		–		1266.9[a]		1267.7[a]		–	
$\nu_2(A_1)$, δ(OCO)	807.0[a]		–		799.3[a]		–		774.3[a]		781.6		–	
	798.7	798.9	798.9	799.0	789.1	789.5	789.4	789.5	766.6	765.8	766.7	765.8	782.8	782.7
$\nu_3(A_1)$, LiO	533.4	533.5	571.0	570.4	532.9	532.4	570.2	569.3	530.7	530.7	566.0	567.9	–	532.1
	520.0		553.7		519.8		553.5		516.3		549.8		–	
$\nu_5(B_2)$, LiO	–	400.2		420.3	–	400.2	–	420.3	–	391.7	–	412.2	–	395.8

[a] Frequencies for "solvated" $LiCO_2$, i.e., $LiCO_2$:CO_2; k_{CO} = 9.07 and k_{LiO} = 0.45 mdyn/Å; k_{LiOC} = 0.34, k_{OLiO} = 0.71, and k_{OCO} = 1.77 mdyn·Å; $k_{LiO,LiO}$ = 0.05 and $k_{CO,CO}$ = 1.55 mdyn/Å; $k_{CO,OCO}$ = 0.73 mdyn.

Scheme I

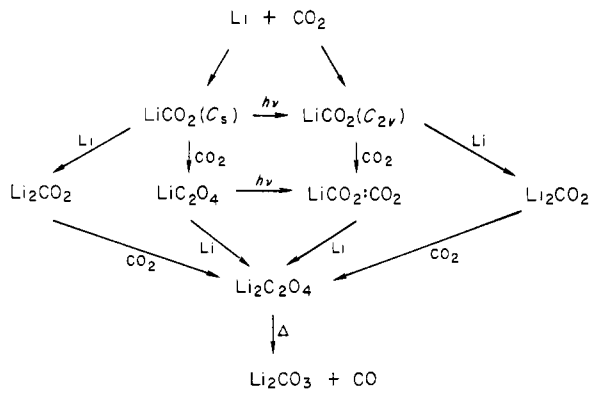

of one or more of the products can be increased or decreased by varying the concentrations of the metal and/or of carbon dioxide. It has been found that both $LiCO_2$ geometrical isomers are produced in very dilute matrices. Li_2CO_2 formation is favored by high metal concentrations, whereas LiC_2O_4 and $LiCO_2$:CO_2 can be obtained only at the high ratio of CO_2:Li of about 25:1. The highest yield of $Li_2C_2O_4$ can be achieved in concentrated matrices. $LiCO_2(C_s)$ and LiC_2O_4 are converted to $LiCO_2(C_{2v})$ and $LiCO_2$:CO_2, respectively, when the matrices are irradiated with the Nernst glower IR source for a few hours. It is found that this photolytic conversion continues to take place but at a slower rate when a quartz filter is used that has an infrared cutoff of ~3000 cm^{-1}. This observation suggests that infrared radiation partially contributes to the conversion of asymmetric to symmetric $LiCO_2$ and LiC_2O_4 to $LiCO_2$:CO_2, possibly through excitation of one of the vibrational modes of each molecule. Heating the matrix to 30 K and cooling it back again also cause the interconversion of $LiCO_2(C_s)$ into $LiCO_2(C_{2v})$.

Thus the chemistry that can take place when Li is allowed to react with CO_2 in excess argon is summarized in Scheme I.

(2) In a Xenon Matrix. Reaction of lithium atoms with carbon dioxide in excess xenon led only to the formation of $LiCO_2(C_{2v})$, Li_2CO_2, and $Li_2C_2O_4$. Thus it appears that xenon does not stabilize the C_s form of $LiCO_2$ which is a precursor to the formation of the new LiC_2O_4 molecule upon addition of CO_2. This might be explained in terms of the larger holes of a xenon matrix, which may allow $LiCO_2(C_s)$ once formed to rearrange to the more stable isomer $LiCO_2(C_{2v})$. On the other hand, the argon matrix may be more capable of quenching the newly formed $LiCO_2(C_s)$ and thus stabilizing this metastable form of $LiCO_2$.

(3) In a Carbon Dioxide Matrix. Only $LiCO_2$ and $Li_2C_2O_4$ are formed when lithium atoms are deposited in a pure CO_2 matrix. The absence of Li_2CO_2 and the presence of $Li_2C_2O_4$ in large amounts suggest that the formation of lithium oxalate in pure CO_2 matrix takes place either through the reaction of Li_2CO_2 with CO_2 or via the dimerization of two $LiCO_2$ in adjacent sites. When the CO_2 matrix is slowly heated, the adduct $LiCO_2(CO_2)_x$ remains present up to 80 K. At 200 K, $LiCO_2$ completely disappears, and only bands associated with $Li_2C_2O_4$ are present. Further heating of the matrix causes the decomposition of $Li_2C_2O_4$ into Li_2CO_3 and CO. The rate of this decomposition reaction has been previously studied.[19] One can summarize the chemistry from 15 to 600 K for Li and CO_2 as follows:

$$Li + xCO_2 \rightarrow LiCO_2(CO_2)_x + Li \rightarrow Li_2C_2O_4 \xrightarrow{T \gg 300\ K} Li_2CO_3 + CO$$

Table III. Comparison between Theoretical and Experimental Teller-Redlich Product Rule for the Ratios of Frequencies (A_1 Symmetry) of Different $LiCO_2(C_{2v})$ Isotopomers

isotopic ratio	theor	exptl
$^6LiCO_2/LiCO_2$	1.0693	1.0700
$^6Li^{13}CO_2/Li^{13}CO_2$	1.0693	1.0675
$LiCO_2/Li^{13}CO_2$	1.0309	1.0305
$^6LiCO_2/^6Li^{13}CO_2$	1.0309	1.0330
$LiCO_2/LiC^{18}O_2$	1.0835	1.0805

(B) Bonding and Structure of $LiCO_2(C_{2v})$. The existence of $LiCO_2$ in two geometrical forms is quite interesting. Spin-restricted Hartree–Fock calculations[26] have predicted the possibility of two geometrical isomers for $LiCO_2$: one has a symmetric structure where the Li interacts equally with the two oxygen atoms while the other has the lithium bonded to one of the two oxygens. Stabilization energies for both isomers were calculated to be almost equal, namely, 0.83 eV for $LiCO_2(C_s)$ and 0.85 eV for $LiCO_2(C_{2v})$.

Table II lists the measured infrared frequencies for the predominant bands assigned to $LiCO_2(C_{2v})$ as well as its "solvated" counterpart $LiCO_2$:CO_2. For such a geometry, one expects six infrared-active modes, five in-plane of A_1 (three) and B_2 (two) symmetries and one out-of-plane of B_1 symmetry. Only frequencies for four in-plane modes have been measured. The assignment of these modes is based on the Teller–Redlich product rule and the ^6Li, ^{13}C, and ^{18}O frequency shifts. Tables III shows the close agreement between the theoretical and experimental product rules for frequencies of A_1 symmetry of different isotopomers. The carbon-13 and oxygen-18 shifts clearly indicate that the three highest frequencies are due to the three CO_2 intraionic modes, namely, the asymmetric and symmetric CO_2 stretches and the δ(OCO) bending mode. The lowest frequency exhibits a large lithium-6 shift of about 37.6 cm^{-1} and thus is assigned to a symmetric Li–O_2 stretching mode.

If one neglects the interaction of CO_2^- with the lithium ion, one can calculate the CO_2^- valence bond angle by using the triatomic molecule approximation and frequencies of the asymmetric stretching mode. Table IV lists the different values for the bond angle calculated by using carbon-13/12 and oxygen-18/16 frequencies measured in argon and xenon matrices. Average bond angles equal to 123 and 125° have been determined for CO_2^- in Ar and Xe matrices, respectively. The bond angle calculated from measured frequencies in Ar matrices is the more accurate of the two since the bands in Ar were sharper and better defined than their counterparts in Xe. The average calculated bond angle compares quite well with the theoretical value obtained

Table IV. Valence Bond Angles (deg) for CO_2^- in $Li^+CO_2^-(C_{2v})$ Using the Triatomic Molecule Approximation

isotopic molecules used in the calculations	matrix	
	Ar	Xe
$LiCO_2/LiC^{18}O_2$	127.8	126.5
$^6LiCO_2/^6LiC^{18}O_2$	131.7	–
$LiCO_2/Li^{13}CO_2$	115.8	123.5
$^6LiCO_2/^6Li^{13}CO_2$	115.1	118.4
av value	122.6	125.0
best matrix value[a]	125.7	125.5
Jordan[26]	124.5	

[a] Bond angle calculated after corrections for anharmonicity, x, have been made: $x = -60.2$ cm^{-1} and $\nu_3/x = -26.1$ in Ar; $x = -9.9$ cm^{-1} and $\nu_3/x = -158.6$ in Xe.

Table V. Comparison between Measured and Calculated Isotopic Frequency Shifts (cm^{-1}) for the Asymmetric Stretching Mode of CO_2^- in $LiCO_2$

isotopomers used in the calculations	measd shift in Ar	measd shift in Xe	calcd shift	calcd shift[a]
$LiCO_2/Li^{13}CO_2$	40.0	41.2	41.3	41.3
$^6LiCO_2/^6Li^{13}CO_2$	40.2	40.5	41.4	41.3
$LiCO_2/LiC^{18}O_2$	27.8	28.1	28.8	28.9
$^6LiCO_2/^6LiC^{18}O_2$	27.4	–	28.8	28.9

[a] Using the triatomic molecule approximation.

by Yoshioka and Jordan (124.5°).[26] It is interesting to note that correction for anharmonicity has raised the calculated angle by 2.7° in Ar and only 0.5° in Xe and thus brought the bond angle in closer agreement with the theoretical value. The anharmonicity, x, calculated for this mode in Ar ($x = -60$ cm^{-1}, $\nu_3/x = -26$) is higher than that for NO_2 ($x = -42$ cm^{-1}, $\nu_3/x = -38.4$).[30]

A more accurate bond angle could have been calculated if the asymmetric (ν_5) Li–O_2 stretching frequency had been observed, as one could then use the Teller–Redlich product rule (B_2 symmetry) and the measured frequencies for different $LiCO_2$ isotopomers. However, calculated isotopic shifts for the ν_4 (B_2) mode with a complete structure and an assumed value for ν_5 agree very well with those obtained from the triatomic molecule approximation. This suggests the validity of this approximation in determining the OCO bond angle. Table V shows a comparison between the measured and calculated frequency shifts, assuming $\nu_5 = 400$ cm^{-1}. The calculated isotopic shifts are consistently higher than the measured shifts, which reflects the fact that these vibrational modes are not totally harmonic.

Normal coordinate analyses have been carried out on $LiCO_2$ (C_{2v}) by assuming the following structural parameters: ∠OCO = 123°, ∠OLiO = 73°, $r_{CO} = 1.260$ Å, and $r_{LiO} = 1.905$ Å. This structure is very close to that calculated by Jordan[26] except for a slightly smaller OCO angle, which was determined from the triatomic molecule approximation for CO_2^- by using the asymmetric C–O stretching frequencies of CO_2^-, $^{13}CO_2^-$, and $C^{18}O_2$. A calculated CO force constant equal to 9.07 mdyn/Å is close to that for the isoelectronic molecule, NO_2 ($k_{NO} = 10.52$[30] or 11.04[31] mdyn/Å). The force constant of NO_2 is greater than that of CO_2^-, which reflects the stronger NO bond. This result is consistent with the shorter NO bond ($r_{NO} = 1.19$ Å).[31] Both molecules have large stretch–stretch interaction force constants (compare $k_{CO,CO} = 1.55$ vs $k_{NO,NO} = 2.44$[30] or 2.14[31] mdyn/Å). The bending as well as the bend–stretch interaction force constants of CO_2^- and NO_2 compare very well ($k_{OCO} = 1.12$ vs. $k_{ONO} = 1.109$, and $k_{OC,OCO} = 0.59$ vs. $k_{ON,ONO} = 0.481$ mdyn/Å). The minimum number of interaction force constants was used in this calculation to obtain the best fit between the measured and calculated frequencies for all the isotopomers of $LiCO_2(C_{2v})$.

(30) D. W. Green, S. D. Gabelnick, and G. T. Reedy, *J. Chem. Phys.*, **64**, 1697 (1976).
(31) G. R. Bird, J. C. Baird, A. W. Jache, J. A. Hodgeson, R. F. Curl, Jr., A. C. Kunkle, J. W. Bransford, J. Rastrup-Andersen, and J. Rosenthal, *J. Chem. Phys.*, **40**, 3378 (1964).

Table VI. Comparison between Observed and Calculated Frequencies (cm^{-1}) for $LiCO_2(C_s)$ Isotopomers in Argon[a]

vibr in-plane mode	$LiCO_2$		$^6LiCO_2$		$Li^{13}CO_2$		$^6Li^{13}CO_2$		$LiC^{18}O_2$		$^6LiC^{18}O_2$		$LiC^{18}O^{16}O$		$LiC^{16}O^{18}O$	
	obsd	calcd	obsd	calcd	obsd	calcd	obsd	calcd	obsd	calcd	obsd	calcd	obsd	calcd	obsd	calcd
ν_1(A′), C=O	1755.7		1756.9		1711.4		1712.2		1722.7		1724.0		–		–	
ν_2(A′), C–O	1750.9	1751.5	1751.2	1751.9	1707.0	1707.0	1708.2	1707.4	1718.3	1717.6	1719.0	1717.9	1723.1	1724.4	1745.8	1745.7
	1221.4	1219.4	1221.7	1222.6	1204.6	1202.7	1205.2	1205.9	1180.3	1177.5	1180.8	1181.3	1198.3	1202.2	1192.9	1193.6
	1208.7		1210.0		1194.0		1194.7		1168.6		–		–		–	
ν_3(A′), δ(OCO)	739.5	739.3	745.5	745.2	730.4	729.3	737.6	736.1	712.8	713.9	719.2	720.5	730.0	730.8	722.8	722.9
ν_4(A′), LiO	611.6		–		608.0		–		606.6		–		–		–	
	599.3	599.0	633.3	633.5	596.3	597.3	629.9	631.0	593.8	592.5	626.7	625.9	–	597.5	–	594.0
ν_5(A′), δ(LiOC)	–	200.0	–	206.9	–	199.5	–	206.4	–	194.3	–	201.4	–	197.6	–	196.6

[a] $k_{C=O} = 12.02$, $k_{C-O} = 9.32$, and $k_{LiO} = 1.46$ mdyn/Å; $k_{OCO} = 1.12$, $k_{LiOC} = 0.29$, and $k_{OCO,OLiO} = -0.16$ mdyn·Å; $k_{OC,OC} = 2.09$, $k_{OC,LiO} = 1.37$, and $k_{C=O,LiO} = 1.30$ mdyn/Å; $k_{OC,OCO} = 0.89$ and $k_{LiO,OCO} = 0.04$ mdyn.

Table VII. Infrared Frequencies (cm^{-1}) for $Li_2CO_2(C_s)$ Isotopomers in Argon and Xenon Matrices

vibr mode	$^6Li_2CO_2$		Li_2CO_2		$^6Li_2{}^{13}CO_2$		$Li_2{}^{13}CO_2$		$^6Li_2C^{18}O_2$		$Li_2C^{18}O_2$	
	Ar	Xe	Ar	Xe	Ar	Xe	Ar	Xe	Ar	Xe	Ar	Xe
ν_1(A′), CO	1447.9	1428.2	1447.9	1426.4	1412.4	1396.3	–	1391.8	1418.7	–	1418.5	1397.9
											1412.6	
ν_2(A′), CO	–	991.9	984.2	988.2	–	971.7	–	965.1	975.2	–	968.8	973.6
											963.2	
ν_4(A′), LiO	–	593.6	565.9	556.9	–	592.9	–	556.4	604.0	–	567.6	553.1
											559.4	

Table VIII. Infrared Frequencies (cm^{-1}) for $LiC_2O_4(C_{2v})$ Isotopomers in Argon

vibr mode	$^6LiC_2O_4$	LiC_2O_4	$^6Li^{13}C_2O_4$	$Li^{13}C^{12}CO_4$	$Li^{13}C_2O_4$	$^6LiC_2{}^{18}O_2{}^{16}O_2$	$^6LiC_2{}^{18}O_4$	$LiC_2{}^{18}O_4$
$\nu(B_2)$, C=O	1969.1	1968.7	1917.0	1952.8	1916.5	1958.0	1937.4	1937.2
$\nu(A_1)$, C-O	1167.8	1159.8	1158.0		1152.3			1118.4

Table II lists the measured vs. calculated frequencies for the in-plane modes of all isotopomers of $LiCO_2(C_{2v})$, assuming the above structure and the force constants (also listed in the footnote of the table). Eight force constants were used to fit 22 observed frequencies. A 0.09% average error in frequency was calculated in this analysis.

(C) Structure of $LiCO_2(C_s)$. Jordan[26] has predicted the possible existence of two geometrical isomers for $LiCO_2$: one has a rhombic structure of C_{2v} symmetry discussed in the previous section, and the second structure has C_s symmetry where the Li is bound to only one oxygen. For such a geometry six infrared-active modes would be expected, five in-plane of A′ symmetry and one out-of-plane of A″ symmetry. The five in-plane modes can be classified as C=O, C-O, and Li-O stretches and two δ(OCO) and δ(LiOC) bends. From the carbon-13 and oxygen-18 isotopic frequency shifts the three highest frequencies have been assigned to C=O and CO stretching and δ(OCO) bending modes. The lowest frequency exhibits a large lithium-6 shift and is thus associated with a Li-O stretching mode. No frequency was observed that could be assigned to the δ(LiOC) bending and/or the out-of-plane mode, which probably lies below the spectrometer's range (400 cm^{-1}). Table VI lists all the predominant measured infrared frequencies assigned to all $LiCO_2(C_s)$ isotopomers. Jordan[26] has predicted a $\angle OCO = 132.4°$, which seems to be reasonable since one expects the bond angle of OCO to be larger in this geometry than in the rhombic structure because of the interaction of Li with only one oxygen. Again one would expect the CO bonding to be close to a double bond for the CO that is not in closest contact with Li, and this is also supported from infrared data as evidenced by the higher frequency measured for $LiCO_2(C_s)$, which lies in the C=O stretching region.

Normal coordinate calculations were carried out using the structure calculated by Jordan[26] for this molecule. Eleven force constants whose values are in the footnote of Table VI were used to fit 30 measured frequencies assigned to the in-plane modes of $LiCO_2(C_s)$ isotopomers. An average error of 0.10% in frequencies was calculated in this analysis. The force constant calculated for the CO bond nearest the Li atom is in the same range as k_{CO} = 9.07 mdyn/Å ($LiCO_2(C_{2v})$) and k_{NO} = 10.52[30] or 11.04[31] mdyn/Å (NO_2) indicating that the bonding is approximately of equal strength in these three molecules. The force constant obtained for the CO bond further removed from the Li atom has a value close to the lower limit of a typical C=O bond. Typical values were also obtained for the other diagonal force constants, namely, k_{OCO} = 0.72 and k_{LiO} = 1.46 mdyn/Å. The value of the k_{LiOC} bending force constant was chosen such that one obtains a low LiOC bending frequency, ν_5 = 200 cm^{-1}. Introduction of large stretch-stretch and stretch-bend interaction force constants was necessary in order to obtain a good fit between the measured and calculated frequencies.

(D) Structure of $Li_2CO_2(C_s)$. Reaction of dilithium or two lithium atoms with CO_2 leads to the formation of Li_2CO_2. Oxygen-18/16 mixed isotopic studies suggest that the two oxygen atoms are not equivalent in this molecule as reflected from the unresolved quartet pattern of the Li_2CO_2 absorption bands. A possible structure for this molecule is that of a perturbed formic acid where the lithium atoms replace the hydrogens and where one of the lithiums may be slightly interactive with the carbonyl oxygen as shown here:

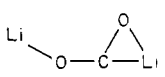

Only three frequencies have been assigned to this molecule, and they are listed in Table VII. The highest two frequencies are due to CO stretching modes since they exhibit large carbon-13 and oxygen-18 isotopic shifts, while the lowest frequency is associated with a Li-O stretching mode because of its large lithium-6 shift. The value of the highest frequency lies considerably lower than that expected for a C=O stretching mode and is further evidence for the interaction of one of the lithiums with the carbonyl oxygen.

Table IX. Infrared Frequencies (cm^{-1}) for $Li_2C_2O_4$ Isotopomers in Argon

vibr mode	$Li_2C_2O_4$	$Li_2{}^{13}C^{12}CO_4$	$Li_2{}^{13}C_2O_4$	$Li_2C_2{}^{18}O_4$
$\nu(B_{3u})$, CO	1662.2	1652.1	1618.5	1634.9
$\nu(B_{2u})$, CO	1315.5	–	–	1277.1
$\nu(B_{2u})$, δ(OCO)	807.0	804.4	799.3	774.3
$\nu(B_{2u})$, LiO	497.7	–	488.6	489.6

Recent theoretical calculations[31] have suggested that the most stable geometry of Li_2CO_2 is indeed the C_s form.

(E) Structures of $LiC_2O_4(C_{2v})$. For the first time LiC_2O_4 has been observed in an inert-gas matrix as a result of the reaction of one lithium atom with two carbon dioxide molecules. Mixed $^{13}CO_2/^{12}CO_2$ study suggests that the two carbon atoms are equivalent. An unscrambled mixed $C^{18}O_2/C^{16}O_2$ (i.e., $C^{18}O^{16}O$ is absent) study further proves the equivalence of the two CO_2 molecules thus supporting the structure proposed for this molecule, which is of C_{2v} symmetry:

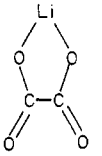

where the lithium is equally interactive with two of the four oxygen atoms. Only frequencies for two modes have been observed for all LiC_2O_4 isotopomers, and they are listed in Table VIII. The higher frequency exhibits large carbon-13 and oxygen-18 shifts and is assigned to a C=O stretching mode while the lower frequency shows a small carbon-13 and a large oxygen-18 shift and is attributed to a C-O stretching mode. The large separation between the C=O and the C-O stretching frequencies indicates a strong Li-O bond since one would expect lengthening of the CO (bonded to Li) and shortening of the CO (free) bonds with respect to the free $C_2O_4^-$ symmetric anion as the metal interacts with the oxygens of the anion.

However, ab initio studies[32] on the structure and stability of $(CO_2)_2^-$ indicate that the interaction between the carbon atoms is quite weak as reflected from a calculated bond order of 0.5. Three different structures of almost equal stabilities have been proposed for this anion. One has four equivalent oxygens in a D_{2h} symmetry, while in a second structure the two oxygens on one of the carbons are twisted 90° of the plane. The third proposed geometry is of C_s symmetry where the CO_2^- anion is interactive with the neutral CO_2 molecule through one of its oxygens. $(CO_2)_2^-(C_s)$ is found to be the most stable structure with a difference of 0.2 and 0.4 eV for $(CO_2)_2^-(D_{2d})$ and $(CO_2)_2^-(D_{2h})$, respectively. It is interesting that the experimental results obtained in this laboratory confirm this prediction since it was shown that $LiC_2O_4(C_{2v})$ is photolytically converted to the "solvated" $LiC_2O_2{:}CO_2$ molecule. However, our mixed $C^{18}O_2/C^{16}O_2/C^{18}O^{16}O$ studies do not suggest that the two oxygens in the CO_2^- in $LiC_2O_2{:}CO_2$ are nonequivalent as proposed from the theoretical work.

(F) Structure of $Li_2C_2O_4(D_{2h})$. Frequencies assigned to lithium oxalate, which is formed upon the co-condensation of lithium with carbon dioxide in an argon matrix, are listed in Table IX. Similar frequencies for $Li_2C_2O_4$ isotopomers measured in a xenon matrix were reported in an earlier publication.[27] This assignment is

(32) Y. Yoshioka and K. D. Jordan, *J. Am. Chem. Soc.*, **102**, 2621 (1980).

Table X. Comparison of Observed Product Band Positions (cm^{-1}) for Residue on Trapping Surface after CO_2 Is Sublimed away from ^6Li and CO_2 Matrix with Reported Frequencies for $Li_2C_2O_4$

vibr mode	obsd frequency[a]	reported frequency[35]
$\nu(B_{3u})$, CO	1655 s	1650 vs
$\nu(B_{2u})$, CO	1315 m	1330 vs
$\nu(B_{2u})$, δ(OCO)	775 w	771 vs

[a] vs, very strong; s, strong; m, medium; w, weak.

further verified by comparing the observed product band positions for the residue left on the trapping surface after CO_2 is sublimed away from a ^6Li and CO_2 matrix with reported frequencies for $Li_2C_2O_4$ as shown in Table X. Two structures of D_{2h} symmetry are possible (I and II) for lithium oxalate molecules where the

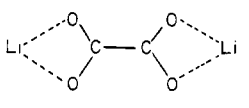

I

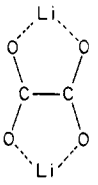

II

two lithiums are at equivalent positions and are equally interactive with two of the four oxygens. These structures seem reasonable as reflected from the values of the frequency assigned to the asymmetric stretching mode since if each lithium were interacting with one oxygen only, the frequency of this mode would have been at a higher value, namely, in the C=O stretching region of $LiCO_2(C_s)$. The second highest frequency is also due to a CO stretching mode, but it is a symmetric one. The third has been attributed to a δ(OCO) bending mode, and the lowest frequency is associated with a Li–O stretching mode. Again these assignments were based on carbon-13, oxygen-18, and lithium-6 isotopic frequency shifts.

X-ray diffraction studies[33] have shown that lithium oxalate has structure II in the solid phase where two of the CO bonds in the trans position are equal and slightly shorter than their counterparts (compare 1.252 vs. 1.264 Å). The carbon–carbon bond length is calculated to be 1.561 Å, which is greater than a typical value for a single bond. The $Li^+\cdots O$ distances vary between 1.931 and 2.071 Å in the crystal structure of $Li_2C_2O_4$. Our observations do not allow us to distinguish between the two structural isomers. However, recently Jordan[32] has carried out preliminary calculations on stabilities and structures of $Li_2C_2O_4$ and has concluded that species II is more stable than I.

Acknowledgment. Funds from the Robert A. Welch Foundation and from the National Science Foundation have supported this study.

Registry No. Li, 7439-93-2; CO_2, 124-38-9; Ar, 7440-37-1; $LiCO_2$, 80480-95-1; Li_2CO_2, 85355-11-9; LiC_2O_4, 85355-12-0; $Li_2C_2O_4$, 553-91-3; ^{13}C, 14762-74-4; ^{18}O, 14797-71-8; Xe, 7440-63-3.

(33) B. Beagley and R. W. H. Small, *Acta Crystallogr.*, **17**, 783 (1964).
(34) K. D. Jordan, University of Pittsburgh, private communications.
(35) M. J. Schmelz, T. Miyazawa, M. Mizushima, T. J. Lane, and J. V. Quagliano, *Spectrochim. Acta*, **9**, 51 (1957).

Asymmetric Synthesis of (+)-2,2,3-Trimethylhex-4-enal via Nucleophilic Attack on η^3-1,3-Dimethylallyl Complexes of Molybdenum

J. W. Faller* and Kuo-Hua Chao

Contribution from the Department of Chemistry, Yale University, New Haven, Connecticut 06511. *Received October 15, 1982*

Abstract: Nucleophilic attack on mixtures of endo and exo isomers of (neomenthylcyclopentadienyl)carbonylnitrosyl(η^3-1,3-dimethylallyl)molybdenum complexes (NM = neomenthyl) provide facile routes to optically pure allylically substituted olefins. A given configuration at the metal center controls the configuration at the allylic center because the exo isomer is attacked preferentially and attack occurs cis to the nitrosyl. Thus, reaction of an enamine of isobutyraldehyde with (*S*)-[NMCpMo(CO)(NO)(η^3-1,3-dimethylallyl)] cation yields (+)-(*R*)-2,2,3-trimethylhex-4-enal upon liberation of the olefin from the complex. The crystal and molecular structure of (*S*)-[(η^5-$C_{15}H_{23}$)Mo(CO)(NO)(η^2-$C_8H_{15}CHO$)] was determined by X-ray crystallographic analysis. The compound crystallizes in the orthorhombic space group $P2_12_12_1$ (D_2^4) (No. 19) with lattice constants a = 10.331 (2) Å, b = 13.571 (3) Å, c = 17.968 (7) Å, and Z = 4. Full-matrix least-squares refinement using anisotropic thermal parameters for the molybdenum and isotropic thermal parameters for the remaining non-hydrogen atoms converged to the final residuals R_1 = 0.069 and R_2 = 0.066.

Since Tsuji's original studies of nucleophilic reactions with (η^3-allyl)palladium complexes,[1] extensive applications to organic syntheses have been developed,[2] particularly by Trost.[3] The use of allylic moieties bound to metal complexes offers the potential of enhanced activity, greater selectivity, and the possibility of control of S_N2 vs. S_N2' attack. The control of regiochemistry and stereochemistry using the palladium systems was exploited originally in stoichiometric reactions, and subsequently, catalytic approaches were developed. The effectiveness of these systems in alkylations suggested that they might be useful in asymmetric synthesis. Considering the high optical yields achieved in asymmetric catalytic hydrogenation using chiral phosphines,[4] these palladium allyls offered a potential route to effective asymmetric allylic alkylations. The stoichiometric reactions using optically active chelating phosphines such as DIOP met with modest success

(1) Tsuji, J.; Takahashi, H.; Morikama, M. *Tetrahedron Lett.* **1965**, 4387; *Bull. Chem. Soc. Jpn.* **1973**, *46*, 1896; *Acc. Chem. Res.* **1969**, *2*, 144–152.
(2) Tsuji, J. **19818** *53*, 2371–2378.
(3) Trost, B. M. *Acc. Chem. Res.* **1980**, 13, 385–93; *Tetrahedron* **1977**, *33*, 265–2649. Trost, B. M.; Strege, P. E.; Weber, L.; Fullerton, T. J.; Dietsche, T. J. *J. Am. Chem. Soc.* **1978**, *100*, 3407–3415. Trost, B. M.; Weber, L.; Strege, P. E. Fullerton, J.; Dietsche, T. J. *Ibid.* **1978**, *100*, 3416–3426, 3426–3434. Trost, B. M.; Verhoeven, T. R. *Ibid.* **1978**, *100*, 3435–3443; **1980**, *102*, 4730–4743. Trost, B. M.; Klun, T. P. *Ibid.* **1979**, *101*, 6756–6758.
(4) Bosnick, B.; Fryzuk, M. D. *Top. Stereochem.* **1981**, *12*, 119–154.

0002-7863/83/1505-3893$01.50/0